THE ASTROPHYSICAL JOURNAL, 494:L1–L4, 1998 February 10

CAN BARYONIC FEATURES PRODUCE THE OBSERVED 100 h^{-1} Mpc CLUSTERING?

DANIEL J. EISENSTEIN,[1] WAYNE HU,[1,2] JOSEPH SILK,[3] AND ALEXANDER S. SZALAY[4]

Received 1997 October 28; accepted 1997 December 9; published 1998 January 19

ABSTRACT

We assess the possibility that baryonic acoustic oscillations in adiabatic models may explain the observations of excess power in large-scale structure on 100 h^{-1} Mpc scales. The observed location restricts models to two extreme areas of parameter space. In either case, the baryon fraction must be large ($\Omega_b/\Omega_0 \gtrsim 0.3$) in order to yield significant features. The first region requires $\Omega_0 \lesssim 0.2\ h$ to match the location, implying large blue tilts ($n \gtrsim 1.4$) to satisfy cluster abundance constraints. The power spectrum also continues to rise toward larger scales in these models. The second region requires $\Omega_0 \approx 1$, implying Ω_b well out of the range of big bang nucleosynthesis constraints; moreover, the peak is noticeably wider than the observations suggest. Testable features of both solutions are that they require moderate reionization and thereby generate potentially observable ($\sim$1 μK) large-angle polarization, as well as subarcminute temperature fluctuations. In short, baryonic features in adiabatic models may explain the observed excess only if currently favored determinations of cosmological parameters are in substantial error or if present surveys do not represent a fair sample of 100 h^{-1} Mpc structures.

Subject headings: cosmology: theory — dark matter — large-scale structure of universe

1. INTRODUCTION

As the study of large-scale structure has pushed to ever larger scales, several data samples have suggested the presence of excess power confined in a narrow region around the 100 h^{-1} Mpc scale. The first such claim was the pencil-beam redshift survey of Broadhurst et al. (1990), in which six concentrations of galaxies separated by a periodic spacing of 128 h^{-1} Mpc were seen. Later work (e.g., Bahcall 1991; Guzzo et al. 1992; Willmer et al. 1994) has confirmed that these overdensities are indeed part of extended structures rather than small-scale anomalies, and new pencil beams show similar behavior (Broadhurst et al. 1995). More recently, the two-dimensional power spectrum of the Las Campanas Redshift Survey (Landy et al. 1996, hereafter LCRS) and the three-dimensional power spectrum of rich Abell clusters (Einasto et al. 1997 and references therein) reveal a narrow peak at similar scales, $k \approx 0.06$ and 0.052 h Mpc^{-1}, respectively.

Other data sets show anomalies on these scales, although they are unable to resolve a narrow feature. Three-dimensional reconstructions based on the angular correlations in the APM survey (Gaztanaga & Baugh 1998) suggest a sharp drop in the power spectrum in this region. Finally, high-redshift C IV absorption lines in quasar spectra were found to be correlated on 100 h^{-1} Mpc scales (Quashnock, Vanden Berk, & York 1996); if this is due to large-scale structure, it indicates greater power than expected. Hence, several different lines of observational inquiry suggest excess power on 100 h^{-1} Mpc scales, perhaps in the form of a narrow peak at wavenumbers $\sim$0.05–0.06 h Mpc^{-1}.

Cosmological models based on collisionless dark matter (e.g., cold dark matter), when combined with power-law initial power spectra, produce smooth power spectra at late times. Such models therefore cannot match the feature described above. However, if baryons are present in significant quantities, the coupling between them and the cosmic microwave background (CMB) photons at redshifts $z \gtrsim 1000$ produces acoustic oscillations near the 100 h^{-1} Mpc scale (see Eisenstein & Hu 1998, hereafter EH98, and references therein).

In this Letter, we consider whether baryonic features in adiabatic models can explain the narrow peak in the power spectrum at 100 h^{-1} Mpc scales. Such models exhibit a power spectrum with a broad global maximum (hereafter the *peak*) at small wavenumbers $k \lesssim 0.05\ h$ Mpc^{-1} and a series of oscillations (hereafter the *bumps*) at larger wavenumbers $k \gtrsim 0.05\ h$ Mpc^{-1} (cf. Fig. 4 below). Therefore, one may attempt to associate either the peak or the first bump with the observed 100 h^{-1} Mpc feature. This yields two disjoint areas of parameter space, as shown in Figure 1. We discuss these separately in §§ 2 and 3.

Throughout this Letter, Ω_0 is the total density of matter relative to the critical density; Ω_b is that of the baryons. The power-law exponent of the initial power spectrum is denoted n. The Hubble constant is written as 100 h km s^{-1} Mpc^{-1}. We assume a cosmological constant to make the universe flat; an open universe would have a power spectrum of identical shape but with a less favorable normalization.

2. LOW-Ω_0 REGION

The region on the left in Figure 1 corresponds to placing the first bump in the region $0.045\ h$ Mpc$^{-1} < k < 0.07\ h$ Mpc^{-1}. The bump shifts to smaller scales (higher k) as Ω_0 increases, as reflected in the left-right limits. We take the bump location to be the position of the corresponding maximum in the oscillatory piece of the transfer function (EH98, eq. [25]).

The lower bound on the baryon fraction Ω_b/Ω_0 comes from the requirement that the amplitude of the bump, as measured using the decomposition of EH98, exceeds 20% in power. Smaller oscillations would not explain the observations (cf. Fig. 4 below, where a 29% oscillation is slightly smaller than that in the data). Very large baryon fractions produce such prominent features that the second bump at $k \approx 0.1\ h$ Mpc^{-1} would have been easily detected (Peacock & Dodds 1994); we conservatively require that the bump amplitude be less than 160%. Note that while lowering h from 0.8 to 0.5 causes the

[1] Institute for Advanced Study, Princeton, NJ 08540.
[2] Alfred P. Sloan Fellow.
[3] Departments of Astronomy and Physics, University of California at Berkeley, Berkeley, CA 94720-3411.
[4] Department of Physics and Astronomy, Johns Hopkins University, Charles and 34th Street, Bloomberg Center, Baltimore, MD 21218.

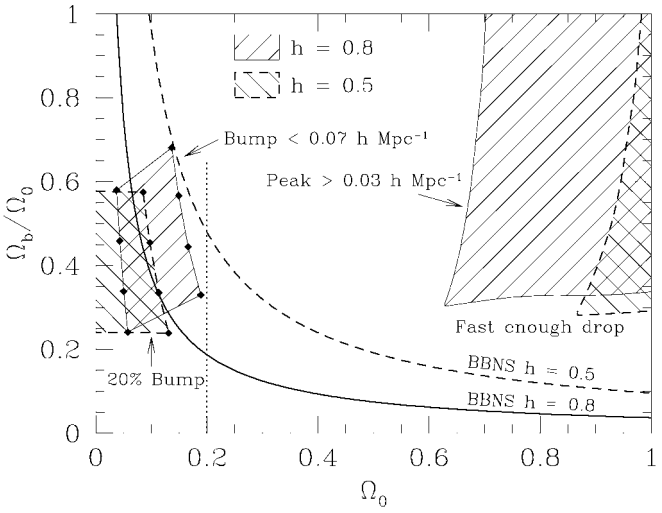

FIG. 1.—Parameter space available for a strong feature at $k \approx 0.05\ h$ Mpc^{-1}. The Ω_0-Ω_b/Ω_0 plane is shown for $h = 0.5$ (*dashed lines*) and $h = 0.8$ (*solid lines*). *Left region*: a bump between $0.045\ h$ and $0.07\ h$ Mpc^{-1} with an amplitude between 20% and 160%, as marked by the filled diamonds at 20%, 40%, 80%, and 160%. *Right region*: the peak at $k \gtrsim 0.03\ h$ Mpc^{-1} with an additional requirement on its prominence (positive HWHM $\lesssim 0.4$ decades [cf. Fig. 3]). The nucleosynthesis constraints of $\Omega_b h^2 = 0.024$ (Tytler et al. 1996) are shown (big bang nucleosynthesis [BBNS]).

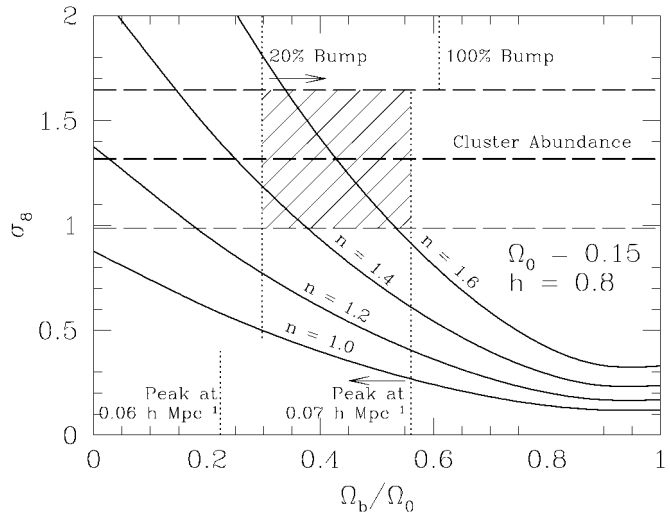

FIG. 2.—The value of σ_8 is shown as a function of the baryon fraction for a *COBE*-normalized flat $\Omega_0 = 0.15$, $h = 0.8$ model. Several different values of tilt are shown (*solid lines*). The value of σ_8 required to match the present-day cluster abundance (*dashed lines*) is taken to be $\sigma_8 = 0.5\Omega_0^{-0.53+0.13\Omega_0}$ (Eke et al. 1996), with 25% variation to reflect errors here and in the *COBE* normalization. The hatched region represents models that satisfy the cluster abundance and bump location while having $\gtrsim$20% power enhancement.

allowed region to shift unfavorably to even lower Ω_0, increasing h to 1.0 only marginally relaxes the bound on Ω_0.

Hence, one is restricted to a low value of Ω_0, approximately less than $0.2\ h$. For $h \approx 0.8$, this does not drastically violate the nucleosynthesis (e.g., Tytler, Fan, & Burles 1996). However, the moderate baryon fraction needed to produce the bumps also causes a significant suppression of power at $k \gtrsim 0.02\ h$ Mpc^{-1}. For a *COBE*-normalized (Bunn & White 1997) and scale-invariant initial spectrum ($n = 1$), the resulting values of the fluctuations on the cluster scale σ_8 are less than 0.5. This is far smaller than the value ($\gtrsim$1.0 for these Ω_0) needed to reproduce the abundance of galaxy clusters.

Adding a significant blue tilt ($n \gtrsim 1.4$) can increase σ_8 enough to satisfy the cluster abundance constraint. We have taken the lowest value in the literature (Eke, Cole, & Frenk 1996) to provide conservative lower bounds on n. We display this situation in Figure 2. In general, larger amplitude features must be balanced by larger tilts. Note that adding a tensor contribution to *COBE* or removing the cosmological constant will decrease the power spectrum normalization and in turn require even higher tilts (White & Silk 1996).

Observational constraints on tilt depend entirely on the range of wavenumbers considered. The limited range of scales available to the *COBE* Differential Microwave Radiometer allows only a weak constraint ($k \approx 10^{-3}\ h$ Mpc^{-1}, $n \lesssim 1.8$; Gorski et al. 1996). Combining *COBE* with degree-scale CMB observations ($k \approx 10^{-2}\ h$ Mpc^{-1}) limits the tilt more severely. However, both constraints may be relaxed if the universe were reionized moderately early. Blue tilts extending to smaller scales are constrained by arcminute-scale CMB observations ($k \sim 1\ h$ Mpc^{-1}, $n \lesssim 2$; Vishniac 1987), the absence of spectral distortions from dissipation of acoustic waves after thermalization ($k \sim 10^4$ Mpc^{-1}, $n \lesssim 1.5$; Hu, Scott, & Silk 1994), and limits on primordial black holes ($k \sim 10^{15}$ Mpc^{-1}, $n \lesssim 1.3$; Green & Liddle 1997). In summary, strong blue tilts that extend from *COBE* to the smallest observable scales are ruled out, but between *COBE* and cluster scales, the situation is less restrictive since the slope may decrease at smaller scales.

The parameter space remaining to the low-Ω_0 region after the peak location, peak amplitude, cluster abundance, and tilt constraints are applied is shown as the hatched regions in Figures 1 and 2.

3. HIGH-Ω_0 REGION

The region on the right in Figure 1 corresponds to placing the peak at $k > 0.03\ h$ Mpc^{-1}. Although the lower limit is well below the observational region 0.05–0.06 h Mpc^{-1}, the peak in these models is sufficiently broad that the exact maximum need not lie directly on the preferred scale to yield an enhancement of power. Figure 1 assumes $n = 1$; adding a blue tilt shifts the peak to higher k, increasing the allowed region. The region for $n = 1.4$ and $h = 0.5$ is very similar to that shown for $h = 0.8$.

The peak is generically much broader than the bump. As the baryon fraction increases, the high-k side of the peak steepens significantly, giving rise to a prominent and asymmetric feature. Two statistics characterizing the width of the peak for an $\Omega_0 = 1$, $h = 0.5$ model are shown in Figure 3. Here one sees that the FWHM always exceeds 0.85 decades in k for $n = 1$ and 0.65 decades for $n = 1.4$. Similarly, the range in k over which the power spectrum drops from its peak to its half-maximum in the high-k direction (positive half-width at half-maximum [HWHM]) always exceeds 0.3 decades for $n = 1$ and 0.25 decades for $n = 1.4$. Adding a blue tilt steepens the low-k side of the peak, thereby decreasing the width.

The observed narrow features are claimed to be inconsistent with the usual low-baryon spectral shape. As shown in Figure 3, the positive HWHM exhibits two plateaus, indicating two distinct morphologies, with a sharp transition near $\Omega_b/\Omega_0 \approx 0.3$. To isolate this deviation from the low-baryon shape, we require that the HWHM be less than 0.4 in Figure 1. While broad, the peaks in these models are systematically sharper

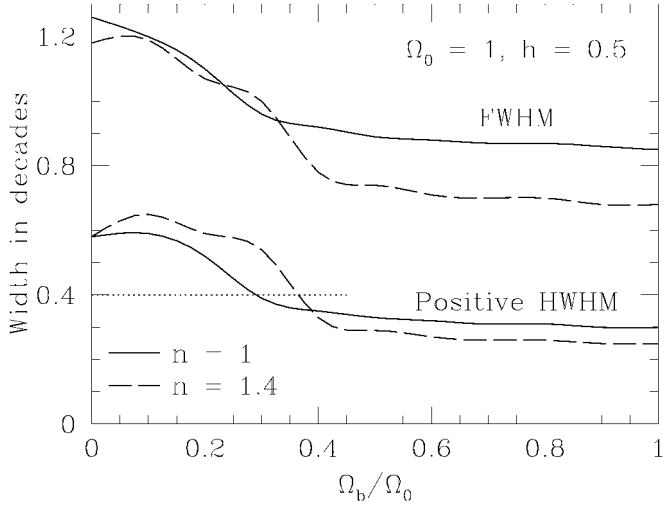

FIG. 3.—The width of the peak of the power spectrum, in decades of wavenumber, for an $\Omega_0 = 1$, $h = 0.5$ model of varying baryon fraction. The FWHM and the positive half-width (HWHM), defined as the range in k between the maximum of the spectrum and its half-maximum in the direction of increasing k, are displayed. We show $n = 1$ models (*solid lines*) and $n = 1.4$ models (*dashed lines*). Increasing h decreases the curves by a small amount. Requiring a HWHM ≤ 0.4 (*dotted lines*) eliminates low-baryon models.

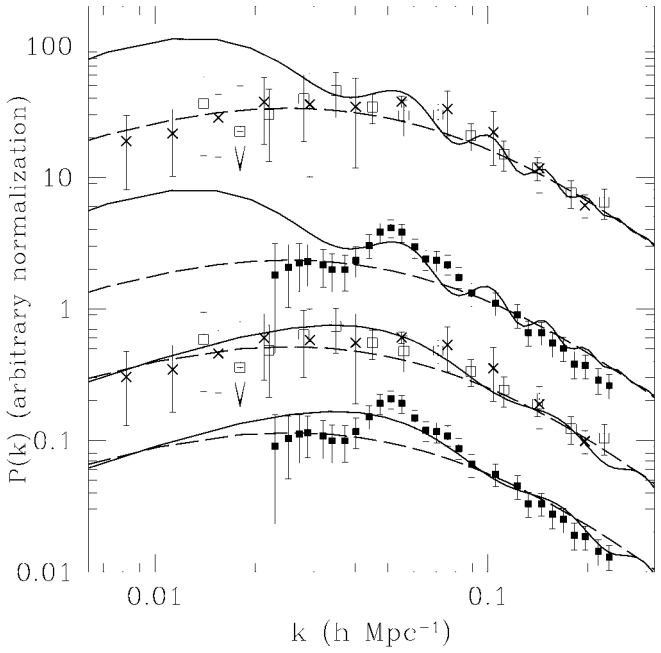

FIG. 4.—Two representative models from the studied regions compared with large-scale structure data. The top two solid curves show an $\Omega_0 = 0.12$, $\Omega_b = 0.04$, $h = 0.8$, $n = 1.6$ model; the bottom two solid curves show an $\Omega_0 = 1$, $\Omega_b = 0.4$, $h = 0.6$, $n = 0.95$ model. The dashed curves are a $\Gamma \equiv \Omega_0 h = 0.25$ zero-baryon model for comparison. The data sets are from the APM survey (Gaztanaga & Baugh 1998) (*crosses*), the compilation of Peacock & Dodds (1994) (*open squares*), and the cluster power spectrum of Einasto et al. (1997) (*filled squares*). All error bars are 2 σ, and only data at $k < 0.25$ h Mpc^{-1} have been plotted. All normalizations are arbitrary. If *COBE*-normalized, partially reionized, and assumed flat, the models have σ_8 of 1.37 (no tensors) and 0.63 (with tensors), respectively.

than those of the low-baryon models against which the observations were compared.

4. DISCUSSION

In Figure 4, we show a representative example from each of the allowed regions and overlay them with observational data sets. The top two curves show an $\Omega_0 = 0.12$, $\Omega_b = 0.04$, $h = 0.8$, $n = 1.6$ model. The first bump is located near $k = 0.06$ h Mpc^{-1} and contains significantly more power than a zero-baryon, $\Gamma \equiv \Omega_0 h = 0.25$ model (*dashed line*). The first bump is prominent and well matched to the Einasto et al. (1997) power spectrum; a similar model would fit the LCRS data. However, the peak at larger scales is even higher, implying that power should continue to rise as we look toward larger scales. This is a generic feature of this region of parameter space—avoided only by enormous blue tilts ($n \gtrsim 2.3$)—and may well be incompatible with the turnover in the power spectrum suggested by the APM survey (Baugh & Efstathiou 1993; Gaztanaga & Baugh 1998). Nonlinearities would likely help to wash out the series of bumps at smaller scales ($k \gtrsim 0.1$ h Mpc^{-1}).

The bottom two curves show an $\Omega_0 = 1$, $\Omega_b = 0.4$, $h = 0.6$, $n = 0.95$ model. Again, the model has excess power on 100 h^{-1} Mpc scales relative to a $\Gamma = 0.25$ model. Because of the high baryon fraction, this model does in fact produce the σ_8 needed to match the $\Omega_0 = 1$ cluster abundance. Of course, the baryon density is in complete violation of the bounds from the nucleosynthesis (Tytler et al. 1996). Due to its large width, the peak feature provides only a marginal, but perhaps adequate, fit to the Einasto et al. (1997) data.

Although unusual, these models need not be at odds with current CMB observations. High baryon fractions tend to enhance the first acoustic peak substantially, and of course blue tilts enhance all power at smaller angular scales. If reionization were not invoked, the models would overproduce degree-scale anisotropies. However, with reionization corresponding to an optical depth of $\tau = 0.75$ for the $\Omega_0 = 0.12$ model and $\tau = 0.5$ for the $\Omega_0 = 1$ model, the degree-scale predictions are suppressed to match current observations (e.g., Smoot 1997). Because of the high baryon content, these values of τ correspond to rather low epochs of reionization, $z_{ri} = 33$ and 13, respectively. Nor does the reionization overproduce secondary anisotropies; we find a Vishniac contribution (Hu & White 1996) across the ATCA band ($l \approx 4500$) of $\Delta T/T = 2.7 \times 10^{-6}$ and 1.9×10^{-6}, respectively, well below the current limit of 1.6×10^{-5} (Subrahmanyan et al. 1993).

Two predictions of these models for the CMB (Fig. 5) are (1) that the second acoustic peak will be quite suppressed compared with the first and third for the high-Ω_0 model, because of the high baryon content, and (2) that the high optical depth will produce substantial CMB polarization levels, approaching band powers of 5×10^{-7} at *COBE* scales, as well as substantial subarcminute temperature fluctuations. These are within reach of the current generation of CMB polarization experiments (Keating et al. 1998) and interferometer experiments, respectively.

In summary, adiabatic cold dark matter + baryon universes with power-law initial power spectra produce the peak found at $k \approx 0.05$–0.06 h Mpc^{-1} only in extreme regions of cosmological parameter space. Placing the first baryonic bump at these wavenumbers requires values of Ω_0 lower than those implied by dynamical mass measurements. This in turn requires extremely large blue tilts and moderate reionization. Avoiding tilts above $n \approx 1.7$ necessitates a cosmological constant $\Lambda =$

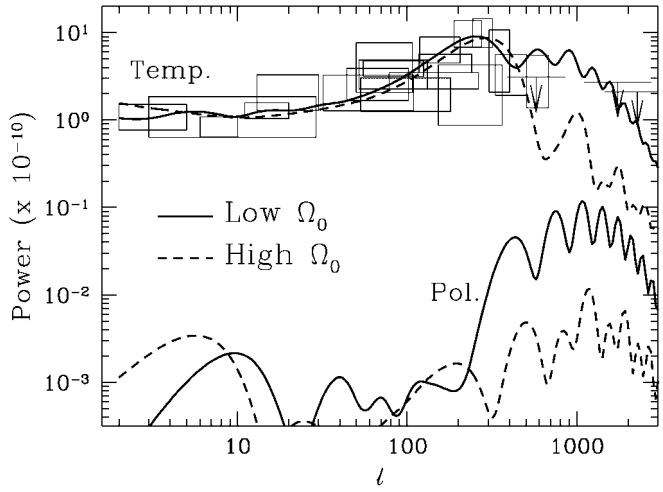

FIG. 5.—CMB temperature anisotropy (including Vishniac effect) and polarization predictions for the two models described in Fig. 4. The models are consistent with the current observational limits (1 σ error boxes on detections and 2 σ upper limits; see, e.g., Smoot 1997 and references therein).

$1 - \Omega_0 > 0.8$ that exceeds limits from gravitational lens surveys (Kochanek 1996). These models may also be in conflict with power spectrum observations at even larger scales ($k \sim 0.02\ h\ \mathrm{Mpc}^{-1}$).

On the other hand, placing the peak of the power spectrum at the observed scale requires high values of Ω_0. Such models need $\Omega_b \gtrsim 0.3$ and, even so, provide a feature that is broader than the observations suggest. Dynamically favored values of Ω_0, say, ~0.3, place the first *valley* of the power spectrum at the desired place!

The question remains as to whether the observations fairly sample the true power spectrum. The narrow width of the observed features may merely indicate that a small number of *k*-modes are dominating the sample. This is more likely if the distribution of amplitudes is non-Gaussian; for example, small nonlinearities in the density field increase the frequency of hot spots in realizations of the power spectrum (Amendola 1994). If the underlying theory has a broad peak around $100\ h^{-1}$ Mpc, different volumes may by chance produce spikes at slightly different locations, with the true width only being recovered in a larger survey. However, some underlying feature will still be required, as shown by the failure of simulations of trace-baryon models to reproduce the observations (LCRS).

Can mildly nonlinear evolution shift the location of the peak in the linear power spectrum? Second-order corrections to the real-space power spectrum (e.g., Jain & Bertschinger 1994) act only to reduce the amplitude of features, although the effects are quite small on the scales in question. Two possible loopholes are coherent effects in redshift space (Szalay et al. 1997) and scale-dependent bias, e.g., if objects tend to trace the scale at which the power spectrum is steepest rather than where it has its maximum.

Finally, one may consider models beyond those treated here. Isocurvature models (e.g., Peebles 1987) produce a sequence of oscillations that are 90° out of phase with those of adiabatic models (Hu & Sugiyama 1996; Sugiyama & Silk 1997). For $\Omega_0 \sim 0.3$, this places the peak of the power spectrum at the intended scale; the first bump is never relevant. Alternatively, one can place a feature directly in the initial power spectrum (Atrio-Barandela et al. 1997). Ongoing redshift surveys should measure the power spectrum to sufficient precision to distinguish between these various explanations of the $100\ h^{-1}$ Mpc excess.

We thank J. R. Bond, Uros Seljak, and Martin White for useful discussions, C. Baugh for supplying his results in electronic form, and the hospitality of the Aspen Center for Physics. The CMB fast package (Seljak & Zaldarriaga 1996) was used to generate numerical transfer functions. W. H. acknowledges support from the W. M. Keck foundation, D. J. E. and W. H. from NSF PHY-9513835, J. S. from NASA and NSF grants, and A. S. Z. from a NASA LTSA.

REFERENCES

Amendola, L. 1994, ApJ, 430, L9
Atrio-Barandela, F., Einasto, J., Gottlöber, S., Müller, V., & Starobinsky, A. 1997, J. Exp. Theor. Phys., 66, 397
Bahcall, N. A. 1991, ApJ, 376, 43
Baugh, C. M., & Efstathiou, G. 1993, MNRAS, 265, 145
Broadhurst, T. J., Ellis, R. S., Koo, D. C., & Szalay, A. S. 1990, Nature, 343, 726
Broadhurst, T. J., et al. 1995, in Wide Field Spectroscopy and the Distant Universe, ed. S. J. Maddox & A. Aragón-Salamanca (Singapore: World Scientific), 178
Bunn, E. F., & White, M. 1997, ApJ, 480, 6
Einasto, J., et al. 1997, Nature, 385, 139
Eisenstein, D. J., & Hu, W. 1998, ApJ, in press (EH98)
Eke, V. R., Cole, S., & Frenk, C. S. 1996, MNRAS, 282, 263
Gaztanaga, E., & Baugh, C. M. 1998, MNRAS, in press
Gorski, K., et al. 1996, ApJ, 464, L11
Green, A. M., & Liddle, A. R. 1997, Phys. Rev. D, 56, 6166
Guzzo, L., Collins, C. A., Nichol, R. C., & Lumsden, S. L. 1992, ApJ, 393, L5
Hu, W., Scott, D., & Silk, J. 1994, ApJ, 430, L5
Hu, W., & Sugiyama, N. 1996, ApJ, 471, 542
Hu, W., & White, M. 1996, A&A, 315, 33
Jain, B., & Bertschinger, E. 1994, ApJ, 431, 495
Keating, B., Timbie, P., Polnarev, A., & Steinberger, J. 1998, ApJ, in press
Kochanek, C. S. 1996, ApJ, 466, 638
Landy, S. D., Schectman, S. A., Lin, H., Kirshner, R. P., Oemler, A. A., & Tucker, D. 1996, ApJ, 456, L1 (LCRS)
Peacock, J. A., & Dodds, S. J. 1994, MNRAS, 267, 1020
Peebles, P. J. E. 1987, Nature, 327, 210
Quashnock, J. M., Vanden Berk, D. E., & York, D. G. 1996, ApJ, 472, L69
Seljak, U., & Zaldarriaga, M. 1996, ApJ, 469, 437
Smoot, G. 1997, preprint (astro-ph/9705135)
Subrahmanyan, R., Ekers, R. D., Sinclair, M., & Silk, J. 1993, MNRAS, 263, 416
Sugiyama, N., & Silk, J. 1997, in preparation
Szalay, A. S., Eisenstein, D. J., Hu, W., & Silk, J. 1997, in preparation
Tytler, D., Fan, X. M., & Burles, S. 1996, Nature, 381, 207
Vishniac, E. T. 1987, ApJ, 322, 597
White, M., & Silk, J. 1996, Phys. Rev. Lett., 77, 4704
Willmer, C. N. A., Koo, D. C., Szalay, A. S., & Kurtz, M. J. 1994, ApJ, 437, 560